Journal of Hydrology 374 (2009) 16–29

Contents lists available at ScienceDirect

Journal of Hydrology

journal homepage: www.elsevier.com/locate/jhydrol

Climate change sensitivity assessment of a highly agricultural watershed using SWAT

Darren L. Ficklin, Yuzhou Luo, Eike Luedeling, Minghua Zhang *

Department of Land, Air and Water Resources, University of California, Davis, CA 95616, USA

ARTICLE INFO

Article history:
Received 25 January 2009
Received in revised form 18 May 2009
Accepted 20 May 2009

This manuscript was handled by P. Baveye, Editor-in-Chief, with the assistance of Adrian Deane Werner, Associate Editor

Keywords:
Watershed modeling
Agricultural watershed
Climate change
SWAT
Water yield
Evapotranspiration

SUMMARY

Quantifying the hydrological response to an increased atmospheric CO_2 concentration and climate change is critical for the proper management of water resources within agricultural systems. This study modeled the hydrological responses to variations of atmospheric CO_2 (550 and 970 ppm), temperature (+1.1 and +6.4 °C), and precipitation (0%, ±10%, and ±20%) based on Intergovernmental Panel on Climate Change projections. The Soil and Water Assessment Tool (SWAT) was used to model the hydrology and impact of climate change in the highly agricultural San Joaquin watershed in California. This watershed has an area of 14,983 km^2 with a Mediterranean climate, resulting in a strong dependence on irrigation. Model calibration (1992–1997) and validation (1998–2005) resulted in Nash–Sutcliffe coefficients of 0.95 and 0.94, respectively, for monthly stream flow. The results of this study suggest that atmospheric CO_2, temperature and precipitation change have significant effects on water yield, evapotranspiration, irrigation water use, and stream flow. Increasing CO_2 concentration to 970 ppm and temperature by 6.4 °C caused watershed-wide average evapotranspiration, averaged over 50 simulated years, to decrease by 37.5%, resulting in increases of water yield by 36.5%, and stream flow by 23.5% compared to the present-day climate. Increasing temperature caused a temporal shift in plant growth patterns and redistributed evapotranspiration and irrigation water demand earlier in the year. This caused an increase in stream flow during the summer months due to decreased irrigation demand. Water yield, however, decreased with an increase in temperature. Increase of precipitation by ±10% and ±20% generally changed water yield and stream flow proportionally, and had negligible effects on predicted evapotranspiration and irrigation water use. Overall, the results indicate that the San Joaquin watershed hydrology is very sensitive to potential future climate changes. Agricultural implications include changes to plant growth rates, irrigation timing and runoff, all of which may affect future water resources and water quality.

Introduction

Fossil fuel consumption has caused an increase in anthropogenic emissions of carbon dioxide (CO_2) and other greenhouse gases (IPCC, 2007). Due to higher concentrations of these gases in the atmosphere, the proportion of solar radiation hitting the Earth that is reflected back into space is reduced, leading to a net warming of the planet (Kalnay and Cai, 2003). Based on the range of emission scenarios presented to the Intergovernmental Panel on Climate Change (IPCC, 2007), CO_2 concentrations are expected to increase from the present day concentration of approximately 330 pm to between approximately 550 and 970 ppm. The magnitude of this increase will depend on future human activities, as well as technological and economic development. For all IPCC scenarios, however, General Circulation Models (GCMs) predict that increases in atmospheric greenhouse gas concentrations will raise surface temperatures. These changes will likely affect the hydrologic cycle. Among the GCMs and emission scenarios used by the IPCC, temperatures in 2100 are expected to be between 1.1 and 6.4 °C higher than temperatures in 1900, accompanied by changes in rainfall intensity and amount (IPCC, 2007). Possible changes in regional and seasonal patterns of temperature and precipitation and their implications for the hydrologic cycle are as yet poorly understood.

An increase of atmospheric CO_2 will directly affect plant transpiration and growth which are inherently tied to the hydrologic cycle. Experimental evidence indicates that stomatal conductance of some plants will decline as atmospheric CO_2 increases, resulting in a reduction of transpiration (e.g., Morison and Gifford, 1983; Morison, 1987; Hendry et al., 1993; Tyree and Alexander, 1993; Field et al., 1995; Saxe et al., 1998; Wand et al., 1999; Medlyn et al., 2001; Wullschleger et al., 2002). Research has also shown that total leaf area of many plant types may increase with

* Corresponding author. Tel.: +1 530 752 4953; fax: +1 530 752 5262.
E-mail address: mhzhang@ucdavis.edu (M. Zhang).

0022-1694/$ - see front matter © 2009 Elsevier B.V. All rights reserved.
doi:10.1016/j.jhydrol.2009.05.016

increased atmospheric CO_2 concentrations (e.g., Wand et al., 1999; Pritchard et al., 1999; Saxe et al., 1998), potentially offsetting the reduction of stomatal conductance.

Much research has been done to elucidate the effects that climate change and increased atmospheric CO_2 concentration will have on watershed processes. Studies have reported that an increase in CO_2 while holding temperature and precipitation constant will cause increases in water yield (e.g., Aber et al., 1995; Fontaine et al., 2001; Chaplot, 2007). Using present day precipitation patterns, studies have shown that higher temperatures lead to increased evaporation rates, reductions in stream flow, and increased frequency of droughts (e.g., Schaake, 1990; Rind et al., 1990; Nash and Gleick, 1991, 1993). Labat et al. (2004) demonstrated that a temperature increase by 1 °C may lead to a global runoff increase by 4% due to increased oceanic evaporation. Kamga (2001) used WatBal, a hydrologic water balance model (Yates, 1996), to show that a 1 and 3 °C temperature increase and a 4–13% change in rainfall intensity would result in variations in annual river fluxes of −3% to +18% in Cameroon. In Africa, Legesse et al. (2003) used the Precipitation-Runoff Modeling System (PRMS) model (Leavesley, 1983) to simulate runoff, predicting a runoff decrease by 30% in response to a 10% decrease in precipitation amount. A 1.5 °C increase in air temperature resulted in a runoff decrease of 15%. In a study of climate change effects on the Missouri River in the USA, Lettenmaier et al. (1999) used output from three transient GCMs and one double CO_2 GCM to evaluate potential effects of climate change on water resources. They estimated that the Missouri River would experience a reduction in stream flow between 6% and 34%, which would greatly impact economic infrastructure along the river. All of these studies indicate that watershed processes may be very sensitive to changes in precipitation, temperature and increased atmospheric CO_2 concentrations. Despite many studies on the effects of climate change, up-to-date quantitative information on the effects of changes in precipitation and temperature on soil and water resources is still scarce.

Anticipating changes in the hydrologic cycle is particularly important for regions with limited water supplies such as the San Joaquin Valley in California. This study will contribute to the collection of studies that characterize potential climate change impacts on water resources in California's Central Valley (e.g., Gleick, 1987; Lettenmaier and Gan, 1990; USBR, 1991; Dracup and Pelmulder, 1993; USEPA, 1997; Miller et al., 1999; Wilby and Dettinger, 2003; Knowles and Cayan, 2002; Zhu et al., 2005). Most of these early studies were subject to the underlying assumption that precipitation would not be affected by regional warming which, based on multiple GCM outputs, may not be accurate (Allen and Ingram, 2002). While all GCM model runs predict rising temperatures for California, the magnitude and direction of changes in precipitation is much less certain (Cayan et al., 2008).

Recent studies incorporate precipitation projections from GCMs, downscaled to a higher resolution for California (e.g., Hay et al., 2000; Miller and Kim, 2000; Brekke et al., 2004; Dettinger et al., 2004; VanRheenen et al., 2004; Maurer and Duffy, 2005; Maurer, 2007). These studies show great variability in projected precipitation for California. A large amount of uncertainty of global precipitation is caused by the structure of GCMs and their underlying assumptions (IPCC, 2001). Consequently, no global climate model should be considered superior to others in predicting California precipitation. Any precipitation projections produced for California under the IPCC CO_2 scenarios should therefore be regarded as equally plausible. This study will thus consider a range of possible precipitation scenarios.

Hydrologic models are often combined with climate scenarios generated from GCMs to produce potential scenarios of climate change effects on water resources. These hydrologic models provide a link between climate changes and water yields through simulation of hydrologic processes within watersheds. Hydrologic models then allow various simulations to be performed based on user needs. Confidence in the results varies greatly and largely depends on the methods and structure of the climate scenario and the hydrologic model. The Soil and Water Assessment Tool (SWAT) (Arnold et al., 1998) was used for this study. SWAT includes approaches describing how CO_2 concentration, precipitation, temperature, and humidity affect plant growth, ET, snow, and runoff generation, and has often been used as a tool to investigate climate change effects. Several case studies of climate change impacts on water resources have used this model (e.g., Hanratty and Stefan, 1998; Rosenberg et al., 1999; Cruise et al., 1999; Stonefelt et al., 2000; Fontaine et al., 2001; Eckhardt and Ulbrich, 2003; Chaplot, 2007; Schuol et al., 2008). SWAT has been used to model portions of the San Joaquin watershed (Flay and Narasimhan, 2000; Luo et al., 2008). The objective of this study was to provide a first estimate of the overall impact of climate on the hydrology of the San Joaquin River watershed, including its impact on irrigation water use by local farmers.

It is important to note that an assessment of the sensitivity of a model to climate change does not necessarily provide a projection of the likely consequences of climate change. However, such studies provide valuable insights into the sensitivity of the hydrological systems to changes in climate (Arnell and Liv, 2001). Wolock and McCabe (1999) also stated that sensitivity studies of temperature and precipitation variations can provide important information regarding the responses and vulnerabilities of different hydrologic systems to climate change, especially in the light of substantial uncertainty of GCM climate projections. The specific objectives of this study were to investigate the sensitivity of hydrologic variables, such as ET, water yield (in this case, synonymous with surface runoff and soil water interflow entering the adjacent stream), irrigation water use and stream flow (rate of stream flow at the watershed outlet which will be affected by irrigation diversions) to climate change. To this end, we computed all hydrologic variables for 16 climate change scenarios (six for present-day scenarios, five for the B1 emissions scenario (low CO_2 concentration) and five for the A1FI emission scenario (high CO_2 concentration)), and compared the results to a 50-year baseline scenario with a present-day climate.

Materials and methods

Description of the study area

The San Joaquin River watershed was selected for this study (Fig. 1). According to the United States Geological Survey (USGS), the watershed consists of four hydrologic units: the middle San Joaquin and lower Chowchilla watersheds (identified by the eight-digit hydrologic unit code 18040001), the middle San Joaquin, lower Merced, and lower Stanislaus River watersheds (18040002), the upper Chowchilla and upper Fresno River watersheds (18040007), and the Panoche and San Luis Reservoir watersheds (18040014).The USGS monitoring site at Vernalis (#11303500; Fig. 1) was chosen as the outlet for the entire watershed. The discharge inlets of the upper San Joaquin, upper Merced, upper Tuolumne, and upper Stanislaus Rivers were defined at the USGS monitoring sites of #11251000, #11270900, #11289650, and #1130200, respectively (Fig. 1). The total area of the watershed is 14,983 km^2, with approximately 66% of the total area in the San Joaquin Valley, 15% in the Coastal Range, and 19% in the Sierra Nevada mountains. The watershed is highly agricultural and includes the majority of agricultural areas in the counties of Stanislaus, Merced, and Madera, and part of San Joaquin and Fresno Counties.

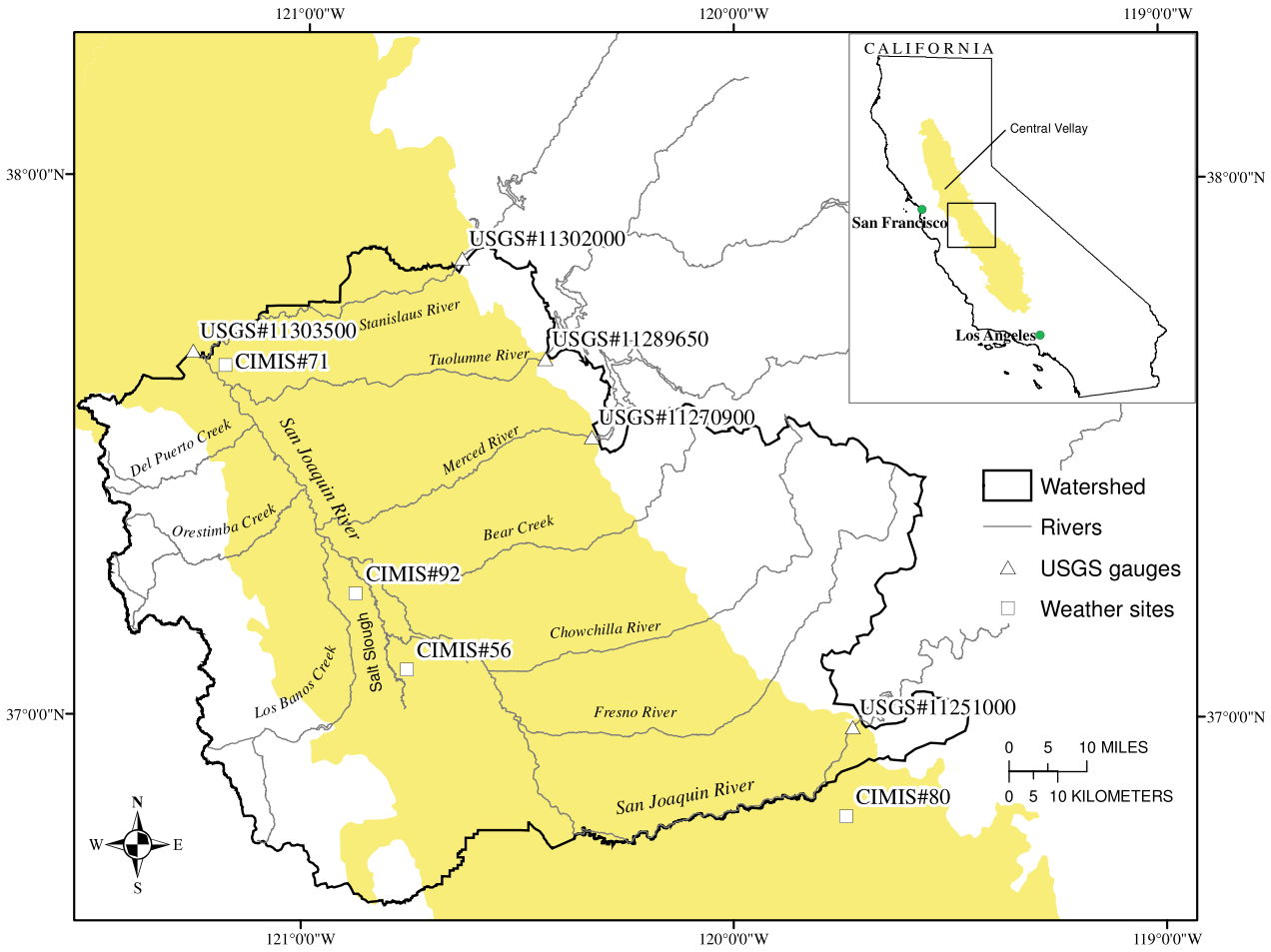

Fig. 1. Study area of the northern San Joaquin Valley watershed (adapted from Luo et al., 2008).

Of the total cropland in the study area, 38% is covered by fruits and nuts, 36% by field crops (corn, tomatoes, pumpkins, watermelon, asparagus, cotton, beans, etc.), 17% by truck, nursery, and berry crops and 4% by grain crops (DWR, 2007).

Agricultural pollution has become a major concern for the watershed (e.g., Foe, 1990; Foe and Connor, 1991; Crepeau et al., 1991; Foe and Sheipline, 1993; Kratzer, 1999). Researchers at the University of California at Davis found that pesticide contamination at 48% of the 237 San Joaquin watershed sampling sites tested exceeded the environmental safety or public health standard maintained by the State of California (CRWQCB, 2000, monitoring data). According to an assessment conducted by the California Regional Water Quality Control Board, at least 127 miles of the San Joaquin River were severely polluted by toxic metals, numerous pesticides, or additional chemicals that promote the growth of algae (SWRCB, 2002). Many portions of the San Joaquin River are listed as Impaired and Threatened Waters by the United States Environmental Protection Agency (USEPA, 2008, Section 303(d)).

The San Joaquin Valley has a Mediterranean climate with hot, dry summers and cool, wet winters. Average rainfall is approximately 200–300 mm with most of the precipitation falling during the period of November–April and negligible rainfall from May to October. Mean daily temperature is approximately 15 °C (NOAA, 2008).

Due to the arid climate, agriculture in the San Joaquin Valley critically depends on irrigation. Farmers in the San Joaquin Valley use a combination of groundwater and surface water to meet their irrigation needs. Irrigation water is mostly developed and delivered by governmental institutions, such as the State Water Project and the Central Valley Project, which sell long-term water contracts. Several irrigation districts such as Modesto or South San Joaquin then deliver the water to the end user via irrigation canals and aqueducts. Farmers manage their own groundwater usage, which to date has not been regulated.

The SWAT hydrological model

SWAT is a hydrologic/water quality model developed by the United States Department of Agriculture–Agricultural Research Service (USDA–ARS) (Arnold et al., 1998; Srinivasan et al., 1998). The main objective of SWAT is to predict the impact of agricultural or land management on water, sediment and agricultural chemical yields in ungauged basins. The model is a continuous-time, spatially distributed simulator of the hydrologic cycle and agricultural pollutant transport at a catchment scale. It runs on a daily time step. Major model components are weather conditions, hydrology, soil properties, plant growth, and land management, as well as loads and flows of nutrients, pesticides, bacteria, and pathogens. A detailed description of SWAT can be found in Nietsch et al. (2005).

In SWAT, a watershed is divided into multiple subwatersheds which are then divided into units of unique soil/land use characteristics called hydrological response units (HRUs). These HRUs are defined as homogeneous spatial units characterized by similar geomorphologic and hydrological properties (Flugel, 1995). In SWAT, HRUs are composed of a unique combination of homogeneous soil properties, land use and slope. For example, a specific HRU land unit may contain a sandy loam, walnut orchards, and a slope of 5%. User specified land cover, soil area, and slope thresholds can

be applied that limit the number of HRUs in each subwatershed. For this study, only land use, soil properties and slopes that comprise over 5% of the subbasin were used for HRU definition. HRU water balance is represented by five storage components: canopy interception, snow, soil profile, shallow aquifer, and deep aquifer. Flow generation is summed across all HRUs in a subwatershed and the resulting flows are then routed through channels, ponds, and/or reservoirs to the watershed outlet.

Predictions of surface runoff from daily rainfall are estimated based on a similar procedure as the CREAMS runoff model (Knisel, 1980). The runoff volume is estimated using the modified SCS curve number method (SCS, 1984), a value that incorporates soil, land use, and management information. The curve number is adjusted at each time step based on the amount of soil water present.

The plant growth component of SWAT utilizes routines for plant development based on plant-specific input parameters summarized in the SWAT plant growth database. From these parameters, SWAT computes plant growth output characteristics such as biomass and leaf area index (LAI). The heat unit theory is used to regulate the plant growth cycle (Boswell, 1926; Magoon and Culpepper, 1932). In this theory, predictions of plant development can be estimated based on the amount of heat absorbed by the plant. Potential plant growth is calculated at each time step of the simulation and is based on growth under ideal growing conditions consisting of adequate water and nutrient supply and a favorable climate.

In SWAT, irrigation may be scheduled by the user or automatically applied in response to a water deficit in the soil. In this study, irrigation in an HRU was automatically simulated by SWAT based on plant-water stress. Depending on the subwatershed, irrigation water was either extracted from the nearby reach or a source outside the watershed. For a given irrigation event, SWAT determines the amount of water available in the source (a stream or river), and the amount of available water is compared to the amount of water needed for the specific irrigation event. Water applied to an HRU is used to fill the soil layers up to field capacity beginning with the soil surface layer and working downward (Nietsch et al., 2005).

SWAT was used because of its capability to model the impacts of future climate conditions. For example, the calculation of ET takes into account variations of radiation-use efficiency, plant growth, and plant transpiration due to changes in the atmospheric CO_2 concentrations, which is essential for any study of CO_2-induced climate change. SWAT allows adjustment terms such as the CO_2 concentration to vary so that the user is able to incorporate GCM projections of atmospheric greenhouse gas concentrations and temperatures into the model simulations. However, SWAT does not allow incremental increases of atmospheric CO_2 concentration. The impact of the increase of plant productivity and the decrease of plant water requirements due to increasing CO_2 levels are considered following Nietsch et al. (2005). For estimation of ET, the Penman–Monteith method must be used for climate change scenarios that account for changing atmospheric CO_2 levels. This method has been modified in SWAT to account for CO_2 impacts on ET levels.

Implications of CO_2 assumptions in SWAT

Many studies using a wide range of plant species have confirmed that increased atmospheric CO_2 concentrations will result in a reduction of leaf stomatal conductance (e.g., Morison and Gifford, 1983; Morison, 1987; Hendry et al., 1993; Tyree and Alexander, 1993; Field et al., 1995; Saxe et al., 1998; Wand et al., 1999; Medlyn et al., 2001; Wullschleger et al., 2002). The most pronounced effect is the effect on the plant growth cycle. In some early work, Morison (1987) suggested that a doubling of CO_2 will lead to a decrease in stomatal conductance of crop by 40%. Since then, other studies have found varying and less pronounced decreases for various plants. Wullschleger et al. (2002) noted that there is a broad range of stomatal conductance responses between different plant species in response to elevated CO_2 levels. Wand et al. (1999) reported a 24% and 29% decrease in stomatal conductance for C3 and C4 grasses, respectively. Field et al. (1995) researched the effect of doubling CO_2 concentration on 23 different tree species. They found an average stomatal conductance decrease of 23%. Medlyn et al. (2001) evaluated 13 long-term, field-based studies on the effects of elevated CO_2 concentrations on tree species. Their results indicated an average decrease of 21% for stomatal conductance, with a stronger effect on deciduous (−24%) than coniferous (−8%).

It has been found that leaf area may also increase under increased CO_2 concentrations. An increase in leaf area would lead to an increase in ET and therefore would affect the hydrologic cycle. Wand et al. (1999) found that a doubling of CO_2 concentration will result in an average leaf area increase of 15% and 25% for C3 and C4 species, respectively. Research conducted by Pritchard et al. (1999) found that leaf area of crop species (37%) increased more than wild, non-woody species (15%) and tree species (14%). SWAT assumes that the leaf area does not increase with increasing CO_2 concentrations.

SWAT 2005 modifies stomatal conductance based on work by Morison (1987). Therefore, doubling CO_2 concentration in SWAT will lead to a 40% reduction in leaf conductance for all plant species. This reduction of conductance is assumed to be linear over the entire range of CO_2 concentrations (Morison and Gifford, 1983). In SWAT, the equation simulating leaf conductance with an increased CO_2 concentration (Easterling et al., 1992) is:

$$g_{CO_2} = g * [1.4 - 0.4 * (CO_2/330)] \quad (1)$$

where gCO_2 is the conductance modified to reflect CO_2 effects; g, the conductance without the effect of CO_2; CO_2 is the atmospheric CO_2 concentration; 330 represents 330 ppm, the present day atmospheric CO_2 concentration. As discussed above, actual stomatal conductance is not linear and is likely to vary with different plant species.

Eq. (1) is for all plant species. Therefore, in watersheds where there are multiple types of land cover not including arable land, the reduction in stomatal conductance may be overestimated. Also, SWAT does not account for leaf area increases due to increased CO_2 concentrations, which could potentially offset the overestimation of stomatal conductance. These are major assumptions in the CO_2-plant growth algorithms in SWAT. Eckhardt and Ulbrich (2003) incorporated variable stomatal conductance and leaf area index (LAI) into SWAT (known as SWAT-G) by compiling plant physiological data from studies researching the influence of increased atmospheric CO_2 concentration. This incorporation, however, has not been adapted into SWAT 2005, the version used in this study.

In this study, the approach used in SWAT 2005 for increased atmospheric CO_2 concentration can be expected to result in an overestimation in the reduction of stomatal conductance and a lack of LAI increase resulting in decreased ET rates and subsequent increases in stream flow and water yield throughout the San Joaquin watershed. Previous research focused solely on evaluating the effects of a doubled atmospheric CO_2 concentration in SWAT report a wide range of impacts on average annual stream flow, including a 0.4% increase in stream flow for the Upper Wind River Basin in northwestern Wyoming (Stonefelt et al., 2000), 16% for the Spring Creek Watershed in western South Dakota (Fontaine et al., 2001), 13–38% for five major Missouri River subwatersheds (Chen, 2001), and 7% for the Walnut Creek Watershed in central Iowa (Chaplot, 2007).

Data collection and analysis

SWAT input parameter values such as topography, landscape, and weather data were compiled using databases from various

state and governmental agencies. Elevation, land use and stream network data were obtained from USEPA's Better Assessment Science Integrating Point and Non-point Sources (BASINS) database (USEPA, 2007). Data included 1:250,000 scale quadrangles of land use/landcover data, 30-m resolution Digital Elevation Models (DEMs), and 1:100,000 scale stream network data from the National Hydrography Dataset (NHD). Cropland and irrigation areas were defined based on the land use survey database developed by the California Department of Water Resources (DWR) during 1996–2004 under the assumption that agricultural land use has not change since the survey was completed. Soil properties were extracted from the 1:24,000 Soil Survey Geographic (SSURGO; USDA, 2007) database based on soil surveys conducted in the study area. Daily precipitation and minimum, and maximum temperature were retrieved from four California Irrigation Management Information System (CIMIS) weather stations in the study area (Fig. 1).

Model initialization and evaluation were based on water monitoring data obtained at gauges within the study area. Stream flow and water quality data for these gauges were collected from the National Water Information System (USGS, 2007) and California Surface Water Database (CEPA, 2007). Monthly average stream flow was aggregated from daily data. Long-term monthly averages were applied where monthly data were missing.

Model calibration and validation

The San Joaquin SWAT model was calibrated using stream flow measured at USGS gauges located on the San Joaquin River and its major tributaries within the study area (Luo et al., 2008). The observed data was split for calibration (1992–1997) and validation (1998–2005) purposes. The longest-running USGS monitoring gauge at the watershed outlet, USGS #11303500 (Vernalis), was selected as the primary location for model calibration and validation. This site receives stream flow from all upstream portions of the study area. Other gauges with shorter records were also used during the model evaluation procedures. Land use and soil properties of the watershed were left unchanged throughout the simulation period.

Full calibration details can be found in Luo et al. (2008). The most sensitive model parameters were chosen in the calibration procedure based on literature review and a preliminary sensitivity analysis (Luo et al., 2008). Initial curve number values in each HRU were estimated based on land use and soil hydrological group via the ArcSWAT interface. The target data range for the curve numbers was established based on the values recommended by USEPA for various crops in the San Joaquin Valley (USEPA, 2002, 2004). Adjustment of the curve numbers within the pre-established range was made to reflect the crop and surface conditions within the study area. As a result, initial curve number values were reduced by 5% of their original value for agricultural HRUs. In the calibrated SWAT model, curve number values for agricultural HRUs ranged from 67 to 87 for the eastern subbasins and 77 to 87 for the western subbasins (Luo et al., 2008). Other parameter modifications were conducted based on the appropriate ranges as defined in the SWAT model documentations. For example, the channel erodibility factor was adjusted for each subbasin individually with factors ranging from 0 to 1.0 (Luo et al., 2008). No changes were made during the validation period.

The simulation generated good results in the comparison with observed stream flow data (Fig. 2). At the Vernalis USGS site, the Nash–Sutcliffe coefficient of efficiency, NS (Nash and Sutcliffe, 1976), for stream flow was 0.95 and 0.94 for the calibration and validation period, respectively (Luo et al., 2008). The NS statistic evaluates the goodness-of-fit of simulated and measured data and ranges from negative infinity to 1 where a value of 1 indicates perfect model accuracy. Full calibration results for selected sampling sites can be found in Table 1. SWAT generated good results in the comparison with measured data, especially for the San Joaquin River and its major eastern tributaries. SWAT also provided satisfactory stream flow prediction for the western San Joaquin tributaries. The lower NS values can be attributed to irrigation, as most of the deviation between predicted and observed stream flow occurred during the irrigation season when diversions and return flow are highest. SWAT simulated wet (1998) and dry (1994) years accurately, indicating that it is a suitable model for evaluating the impact of climate change.

Scenarios of CO_2 concentration, precipitation, and temperature changes

Assuming accurate estimates of the hydrologic cycle components, SWAT was used to evaluate the impact of changes in climate and atmospheric CO_2 concentration. The different scenarios

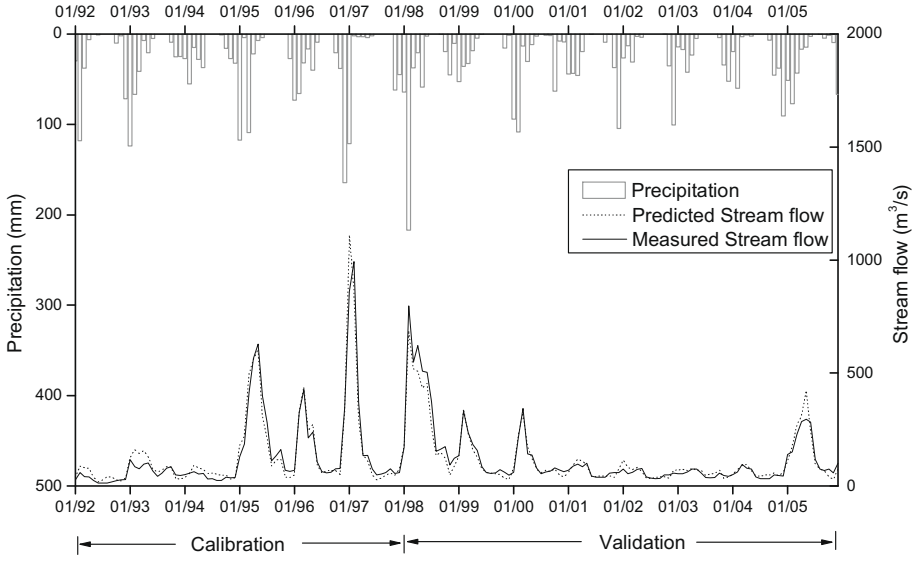

Fig. 2. Observed and predicted monthly stream flows for the San Joaquin River at Vernalis (USGS site #11303500) and monthly precipitation observed in Modesto, CA (adapted from Luo et al., 2008).

Table 1
Calibration and validation statistics for the San Joaquin River and its tributaries (from Luo et al., 2008). NS is the Nash–Sutcliffe coefficient, R^2 is the coefficient of determination and RMSE is the root mean square error ($m^3\ s^{-1}$).

Tributary or river sites	Calibration (1992–1997)			Validation (1998–2005)		
	NS	R^2	RMSE	NS	R^2	RMSE
Merced River	0.83	0.87	10.20	0.67	0.78	8.80
San Joaquin River at Newman	0.91	0.94	40.60	0.88	0.90	38.60
Orestimba Creek	0.50	0.68	1.20	0.49	0.51	1.70
San Joaquin River at Crows Landing	0.88	0.89	36.00	0.82	0.87	25.70
Del Puerto Creek	0.67	0.71	0.40	0.52	0.56	0.70
Tuolumne River	0.98	0.99	8.70	0.99	0.99	4.60
Stanislaus River	0.98	0.98	4.80	0.95	0.96	4.60
San Joaquin River at Vernalis	0.94	0.94	44.70	0.95	0.95	31.10

selected for this study are based on the IPCC Special Report on Emission Scenarios (SRES) (2001) and The Physical Science Basis (2007). The reports describe divergent projections of future atmospheric CO_2 concentration and climate and their underlying uncertainty. Depending on the greenhouse gas emission scenario, atmospheric CO_2 is expected to increase from the current concentration of 330 ppm to between approximately 550 and 970 ppm by the end of the 21st century (IPCC, 2001). We chose the scenarios with the highest (A1FI scenario – 970 ppm by 2100) and lowest (B1 scenario – 550 ppm by 2100) projected CO_2 concentrations for this study. The A1FI scenario assumes a future world of very rapid economic growth, global population that peaks in mid-century and declines thereafter and rapid introduction of new and more efficient technologies. The B1 scenario, in contrast, corresponds to a future of low economic growth and fossil fuel independency. GCMs vary in their predictions of rainfall over the 21st century, and therefore arbitrary scenarios (0%, ±10%, and ±20%) were selected to bracket the range of possible outcomes. Table 2 shows all climate change sensitivity scenarios used in the SWAT simulations.

Daily rainfall amount, minimum (T_{min}) and maximum (T_{max}) daily temperatures were estimated over a 50-year simulated period using the LARS-WG stochastic weather generator (available from http://www.rothamsted.bbsrc.ac.uk/mas-models/larswg/download.php). LARS-WG was chosen over the weather generator included in SWAT, WXGEN, so that the generated data could be manipulated for climate change scenarios before SWAT input. Also, LARS WG was found to produce better precipitation and minimum and maximum temperature results for diverse climates than other weather generators (Semenov et al., 1998). LARS-WG is based on the weather series generator described in Racsko et al. (1991). It utilizes semi-empirical distributions for the lengths of wet and dry day series, and daily precipitation. Daily minimum and maximum temperatures are considered as stochastic processes with daily means and daily standard deviations depending on the wet or dry status of the day. LARS-WG is widely used for climate change studies (e.g., Semenov and Barrow, 1997; Semenov et al., 1998; Luedeling et al., in press). Input data for LARS-WG consisted of CIMIS climate data collected at four weather stations within the study area (Fig. 1).

Table 2
Climate change sensitivity scenarios used for SWAT simulations. The white rows refer to present-day climate perturbations, the light grey rows refer to the B1 scenario and the dark grey rows refer to the A1FI scenario.

Scenario	CO_2 conc. (ppm)	Temperature (°C)	Precipitation (%)
Reference	330	0	0
1	330	1.1	0
2	330	6.4	0
3	330	0	10
4	330	0	20
5	330	0	−10
6	330	0	−20
7	550	1.1	0
8	550	1.1	10
9	550	1.1	20
10	550	1.1	−10
11	550	1.1	−20
12	970	6.4	0
13	970	6.4	10
14	970	6.4	20
15	970	6.4	−10
16	970	6.4	−20

The remaining climate data, solar radiation, and relative humidity, required for SWAT simulation was generated by the WXGEN weather generator (Sharpley and Williams, 1990) included in SWAT. WXGEN uses rainfall and temperature data of each scenario based on the assumption that the occurrence of rain on a given day has a major impact on the relative humidity and solar radiation on that day. For example, generated relative humidity values are adjusted for wed or dry conditions based on the number of wet or dry days in a month.

To address the inconsistencies between the two weather generators, we compared generated results for precipitation, minimum and maximum temperature, and solar radiation. Wind and relative humidity cannot be generated in LARS WG and thus cannot be compared. The comparisons show that LARS WG and WXGEN were both successful at generating climate variables close to the observed values. The coefficients for determination (R^2) for generated precipitation, minimum and maximum temperature, and solar radiation against observed values were above 0.90 for both weather generators, suggesting that the discrepancies between the two weather generators were minor.

All climate change scenarios were run for a 50-year time period (Table 2). Each climate change component (CO_2 concentration, temperature, and precipitation) were increased (or decreased for precipitation) for the entire 50-year time period. For example, a scenario may have a 550 ppm CO_2 concentration, 1.1 °C increase and a 10% precipitation decrease, all of which are simulated for 50 years. The data will then be summarized by annual and monthly averages with respect to the present-day simulation. *T*-tests were done to determine if the climate scenarios and the present-day scenarios are statistically different from each other.

Due to the 50-year time period, adjustment was done for various input parameters needed for SWAT. Long-term monthly averages were used for dam releases into the watershed. Land use/landcover was assumed to remain unchanged throughout the simulation. Irrigation and fertilization were changed according to the automatic algorithm included in SWAT to simulate a reasonable plant growth cycle under various climate conditions.

Results

Characteristics of the baseline scenario

Simulated mean annual rainfall for all climate stations during the baseline 50-year simulated period was 295.4 mm, approximately 17 mm larger than the observed regional CIMIS average. This over-

Table 3
Average monthly hydrologic component values for the reference scenario.

Hydrologic variable	January	February	March	April	May	June	July	August	September	October	November	December
Water yield (mm)	12.2	20.2	19.8	12.2	6.2	1.8	0.7	0.4	0.3	3.0	2.7	7.6
ET (mm)	21.5	31.5	49.5	52.1	64.2	73.1	53.0	35.6	21.6	15.9	15.4	13.2
Irrigation use (mm)	15.0	14.8	24.0	31.4	51.4	101.3	112.4	76.7	44.9	22.1	36.5	4.1
Stream flow ($m^3 s^{-1}$)	157.3	261.3	226.1	191.3	154.6	61.1	28.7	19.1	24.8	55.3	38.2	88.7

estimate is likely due to the large yearly variations in California rainfall (LaDochy et al., 2007). The minimum and maximum simulated yearly rainfall amounts were 127.5 and 541.8 mm, respectively. Maximum daily precipitation was 100.2 mm. The average minimum and maximum daily temperature was 7.78 and 23.8 °C, respectively. Based on our simulation design, model simulation under the baseline scenario was expected to predict comparable hydrological results with observations during 1990–2005. Average predicted stream flow at the watershed outlet (USGS gauge #11303500) was 108.3 $m^3 s^{-1}$ for the reference 50-year simulation period, comparable to the observed average stream flow rate of 115.5 $m^3 s^{-1}$ during 1990–2005. The long-term monthly simulated stream flow averages also corresponded well with observations from 1990 to 2005, indicated by a NS coefficient of 0.70.

CO_2, temperature, and precipitation sensitivity scenarios

Water yield

Present day scenario. Overall, average annual water yield decreased with an increase in temperature and a decrease in precipitation (Table 4). Concurrently, average annual water yield increased with an increase in precipitation. The largest relative increase in average annual water yield was 46.1% with a 20% precipitation increase. The largest decrease was 38.4% with a 20% precipitation decrease. Average monthly water yield results display similar trends as the average annual water yields (Fig. 3). Increasing and decreasing precipitation increased and decreased average monthly water yield for all months, respectively. Increasing temperature (1.1 and 6.4 °C) also decreased water yield, with a 6.4 °C increase resulting in a larger decrease.

B1 Emission scenario. Mean annual water yield was significantly different compared to the present-day scenarios (Table 5). Water yield increased with a precipitation increase. A 0% precipitation increase resulted in a 1.6% increase in average annual water yield. The largest increase was 50.4% with a 20% precipitation increase, and the largest decrease was 37.9% with a 20% decrease in precipitation. Average monthly water yield results exhibited similar trends as the annual water yields (Fig. 3). The largest increase and decrease in monthly water yield occurred during the month of May with an increase and decrease of precipitation by 20%, respectively. Increasing temperature by 1.1 °C did not vary water yield immensely, with all relative increases or decreases below 6%.

A1FI Emission scenario. Average annual water yield significantly changed under the A1FI scenario, increasing for all precipitation scenarios but the 20% precipitation decrease scenario, for which annual water yield decreased by 17.2% (Table 5). The largest increase was 94.5% occurring with a 20% precipitation increase. Generally, average monthly water yield resulted in significant changes for each month, with June showing the largest increase (Fig. 3). The 0%, 10%, and 20% precipitation increases resulted in increases for every month while a 10% precipitation decrease resulted in an increase in water yield for January–August only. A 20% precipitation decrease resulted in water yield decreases throughout the year except June, when water yield increased by 4.3% compared to the baseline scenario.

Evapotranspiration

Present day scenario. Increasing temperature caused an increase in average annual ET relative to the baseline scenario, with a 6.4 °C increase causing a greater ET increase (Table 4). Increasing and decreasing precipitation amounts increased and decreased ET, respectively. The largest increase was 4.0% with a 20% precipitation increase. The largest decrease was 5.4% with a 20% precipitation decrease. Increasing temperature caused the average monthly ET to vary significantly with season, with an increase occurring in the spring months and a decrease in the summer months (Fig. 4). For example, a 6.4 °C increased resulted in a 61.5% ET increase in April and a 50.7% decrease in July. The same effect occurred for a 1.1 °C increase; however, the effect was more subdued with an 8.8% increase in May and a 20.3% decrease in September. The precipitation scenarios did not increase or decrease ET above a 10% relative change.

B1 Emission scenario. Increasing CO_2 concentration and temperature caused a relative decrease in ET for all precipitation scenarios (Table 5). The largest relative decrease was 13.1% and occurred with a 20% decrease in precipitation, and the smallest decrease was 4.7% with a 20% increase in precipitation. Average monthly ET showed seasonal differences with an increase of CO_2

Table 4
Average annual percent change compared to the reference scenario of water yield, evapotranspiration (ET), irrigation water use and stream flow in response to assumed changes in temperature and precipitation at constant atmospheric CO_2 concentration of 330 ppm.

CO_2 conc. (ppm)	Temperature (°C)	Precipitation (mm)	Water yield (mm)	ET (mm)	Irrigation water use (mm)	Stream flow ($m^3 s^{-1}$)
Baseline scenario (absolute values)						
	Modern conditions		85.4	437.7	224.4	108.9
Climate change scenarios (changes relative to baseline scenario)						
	Temperature (°C)	Precipitation (%)	Water yield (%)	ET (%)	Irrigation water use (%)	Stream flow (%)
330	+1.1	0	−3.4	0.4	−0.5[a]	−2.4
330	+6.4	0	−15.6	2.8	−0.8[a]	−11.9
330	0	+10	22.0	2.2	−0.7	8.0
330	0	+20	46.1	4.0	−1.0	16.6
330	0	−10	−20.3	−2.5	0.4	−7.4
330	0	−20	−38.4	−5.4	1.2	−14.3

[a] Represents a lack of significant difference from the reference scenario at $\alpha = 0.05$.

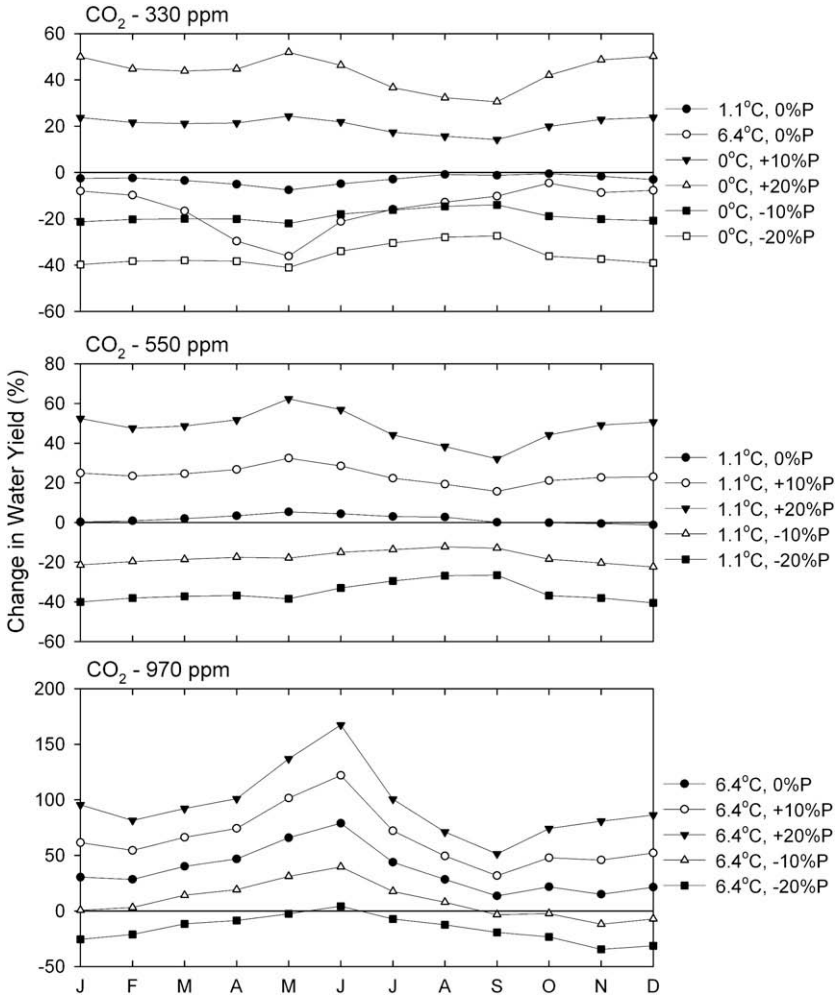

Fig. 3. Change in average monthly water yield relative to the reference scenario.

Table 5
Average annual percent changes for all hydrologic components in comparison to the present-day reference scenario under temperatures and atmospheric CO_2 levels predicted by the B1 and A1FI greenhouse gas emission scenarios of the IPCC. Expected changes in water yield, evapotranspiration (ET), irrigation water use and stream flow are shown for both IPCC scenarios and five precipitation scenarios (+0%, +10%, +20%, −10%, and −20%).

Precipitation scenario	Water yield	ET	Irrigation water use	Stream flow
Baseline scenario (atm. CO_2, temperature, and precipitation at modern levels)				
+0%	85.4 mm	437.7 mm	524.2 mm	108.9 m^3 s^4
IPCC emission scenario B1 (atm. CO_2 = 550 ppm; mean temperature +1.1 °C) change relative to baseline scenario (%)				
+0%	+1.6	−8.1	−15.3	+2.2
+10%	+24.9	−6.2	−15.9	+10.7
+20%	+50.4	−4.7	−16.3	+19.7
−10%	−19.3	−10.4	−14.6	−5.4
−20%	−37.9	−13.1	−13.7	−12.6
IPCC emission scenario A1FI (atm. CO_2 = 970 ppm; change relative to mean temperature +6.4 °C) baseline scenario (%)				
+0%	+36.5	−37.5	−58.3	+23.5
+10%	+65.0	−36.5	−58.8	+32.7
+20%	+94.5	−35.7	−59.1	+42.3
−10%	+8.8	−38.6	−57.9	+14.8
−20%	−17.2	−39.7	−56.9	+5.7

concentration (Fig. 4). The spring months (March–May) showed smaller relative decreases than the late summer/early fall months (July–September). April and May were the only two months that showed a relative increase in ET, and these increases occurred when precipitation was held constant or increased. A decrease in precipitation resulted in a relative ET decrease throughout the year. The largest monthly decrease for all scenarios occurred in September.

A1FI Emission scenario. Average annual ET decreased for every precipitation scenario (Table 5). The largest relative decrease was 39.7% for a 20% decrease in precipitation, and the smallest decrease

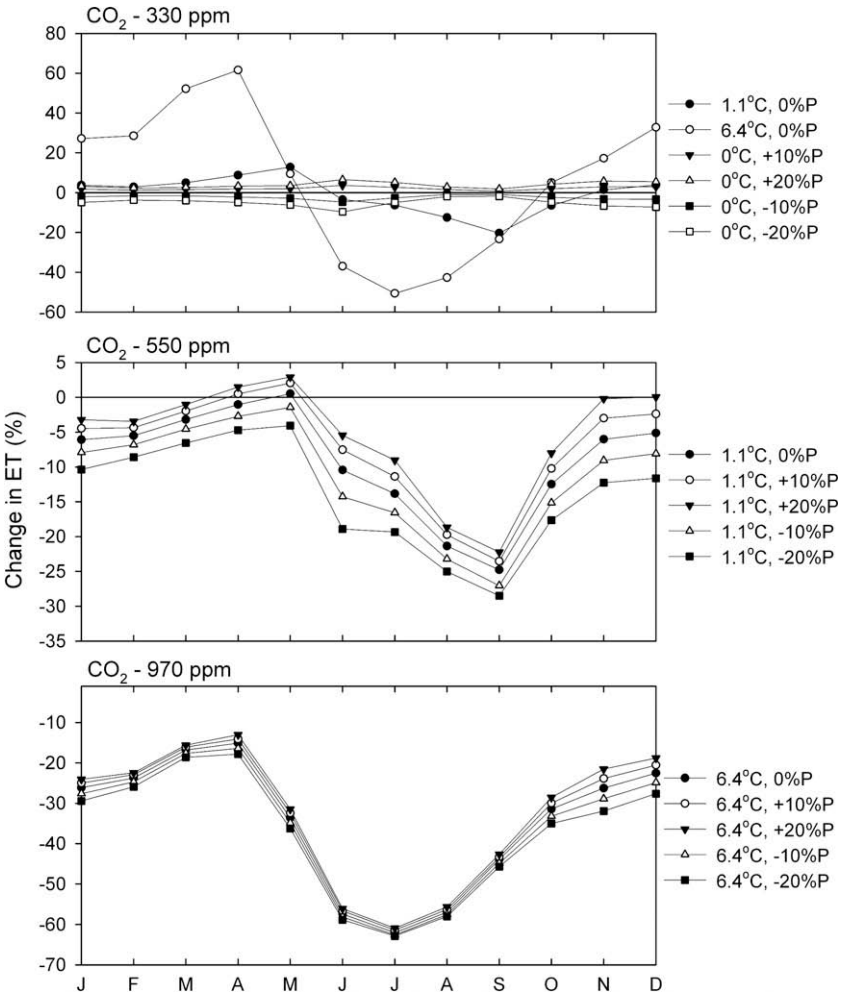

Fig. 4. Change in average monthly ET relative to the reference scenario.

was 35.7% with a 20% precipitation increase. Average monthly ET exhibited strong seasonal differences with a 970 ppm CO_2 concentration (Fig. 4). For example, the smallest decrease occurred in April, while the largest decrease occurred in July, exhibiting strong spring and summer trends. All precipitation scenarios also exhibited these seasonal trends. Average relative ET change for the precipitation scenarios did not vary much between precipitation scenarios, as the largest difference between the largest and smallest change was approximately 10%.

Irrigation water use

Present day scenario. Increasing temperature by 1.1 and 6.4 °C caused slight (statistically insignificant at $p > 0.05$) decreases in average annual irrigation water use by 0.5% and 0.8%, respectively (Table 4). Increasing and decreasing precipitation also caused slight changes in average annual irrigation water use, with an increase in precipitation resulting in a decrease and vice versa. Average annual irrigation water use never varied above or below 1.2%, implying that under present-day temperatures irrigation use does not greatly depend of precipitation. For average monthly irrigation water use, the temperature scenarios showed large deviation from the baseline scenario, while the precipitation scenarios showed little change (Fig. 5). As previously mentioned, increasing the temperature caused a shift in the maximum relative change. Peak average monthly irrigation water use shifted from June to May with a 1.1 °C increase and from June to April with a 6.4 °C increase.

B1 Emission scenario. Increasing CO_2 concentration caused a relative decrease in irrigation water use (Table 5). The results from the scenarios exhibited little variation, with the largest relative decrease being 16.3% in response to a 20% precipitation increase and the smallest decrease being 13.7% caused by a 20% decrease in precipitation. Average monthly irrigation water use showed significant variation from month to month (Fig. 5). The results show a seasonal effect with an increase or slight relative decrease in the spring months (March–May) and a large decrease in the summer months (June–September). September exhibited the largest overall irrigation water use decrease with approximately a 30% decrease for all scenarios. All scenarios resulted in an increase in irrigation water use in December. This increase in December ranged from 4.26 to 4.69 mm, a slight change from the reference December value of 4.14 mm (see Table 3).

A1FI Emission scenario. Increasing temperature and CO_2 concentration had significant effects on average annual irrigation water use, with a minimum decrease of 56.9% with a 20% precipitation decrease (Table 5). The maximum relative decrease of annual irrigation water use was 59.1% with a 20% precipitation increase. Average monthly irrigation water use for each precipitation scenario exhibited a decrease for every month but December, where each scenario showed a relative increase (Fig. 5). Results from the other months exhibit seasonal variation with a lower relative decrease in irrigation water use during the months of

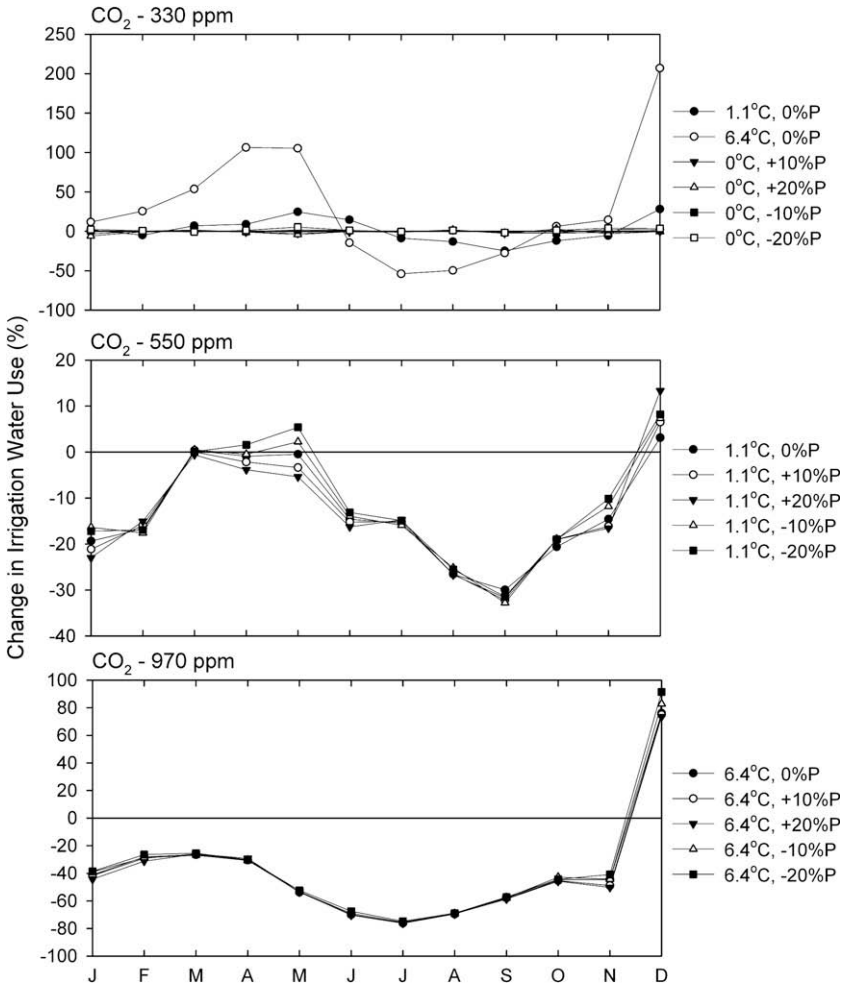

Fig. 5. Change in average monthly irrigation use relative to the reference scenario.

February–April and a higher relative decrease during the months of June–August. The maximum relative decrease was 76.2% and occurred in July with a 20% precipitation increase. Variation of relative changes compared to the baseline scenario was very small among different precipitation scenarios.

Stream flow

Present day scenario. As expected, average annual stream flow rates generally increased with an increase in precipitation and decreased with a decrease in precipitation (Table 4). Increasing temperature by 1.1 and 6.4 °C decreased average annual stream flow rates by 2.4% and 11.9%, respectively. The maximum decrease was 14.3% and occurred with a 20% precipitation decrease. Increasing temperature by 1.1 and 6.4 °C caused average monthly stream flow rates to decrease in the spring months (March–June) and increase in the summer months (July–September) (Fig. 6). Increasing temperature by 6.4 °C affected stream flow rates much more than increasing temperature by 1.1 °C. For example, in August stream flow rates increased by 69.8% with a 6.4 °C increase, while a 1.1 °C increase increased stream flow rates by only 6.2%. Increasing or decreasing precipitation generally changed average annual stream flow rates proportionally, with negligible changes in July, August, and September.

B1 Emission scenario. For these scenarios, the average annual stream flow rates showed similar results as the present-day stream flow rate scenarios (i.e., an increase in precipitation caused an increase in stream flow rates) (Table 5). The maximum relative increase was 19.7% when precipitation was increased by 20%. The minimum relative increase was 12.6% occurring when precipitation was decreased by 20%. Average monthly stream flow rates showed similar trends as the present-day scenarios during the months of November–June (Fig. 6). The remaining months exhibited a very different trend, showing average monthly stream flow rates increases for all precipitation scenarios. September resulted in the largest average monthly stream flow rate increases with 30–33% increases for all scenarios. The largest decrease was 19.3% in December for a 20% precipitation decrease.

A1FI Emission scenario. Average annual stream flow rates increased for all precipitation scenarios (Table 5). The largest increase was 42.3% with a 20% precipitation increase and the smallest decrease was 5.7% with a 20% precipitation decrease. Average monthly stream flow rates generally increased for all months (Fig. 6). The only decreases were found for the months of November–March with decreases in precipitation. Relative to the other months, there were large stream flow rate increases for the months of June–September. The largest increase was in July, where the largest and smallest increases were 191.9% and 170.8%, respectively.

Discussion

The effect of elevated temperature on the hydrologic cycle over the study area manifested itself by a shift of the crop growth cycle.

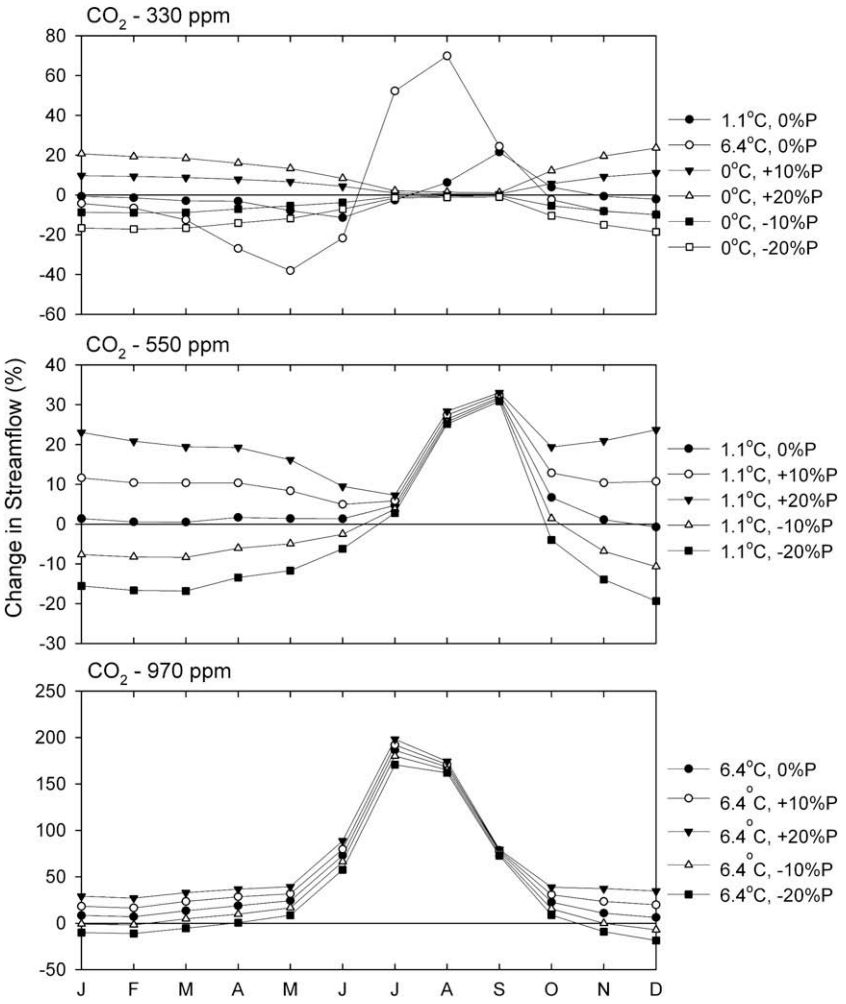

Fig. 6. Change in average monthly stream flow relative to the reference scenario.

Temperature is one of the most important factors governing plant growth. Each crop has its own temperature range, i.e., its minimum, optimum, and maximum for growth. SWAT includes a crop database used for temperature stress estimation, which defines a minimum, optimum, and maximum temperature for each crop. For orchard crops for example, the temperatures are 7, 20, and 33 °C, respectively. For any plant, a base temperature must be reached before any growth takes place. Above the base temperature, the higher the temperature the more rapid the growth rate of the plant. Once the optimum temperature is reached, the plant's growth ceases. With an increasing temperature this base temperature will be reached much sooner in the growing season and thus the plant growth cycle will be shifted. For instance, comparison of simulated crop growth curves indicated that at elevated temperature the watershed-wide average LAI with elevated temperature peaked ahead up to 2 months relative of the reference scenario (Fig. 7).

Increased temperature affected all of the hydrologic components in the study area. Although the annual total amounts of irrigation water and ET rates only changed slightly (<5%) under higher temperature, simulated results showed great monthly variations compared to the reference scenario. Irrigation water use and ET increased during the winter months and decreased during the summer months, showing the effect of plant growth changes. Given the same amount of precipitation, water yields from the study area were related to irrigation water use, and significantly reduced by increased ET. Consequently, the predicted annual water yields over the studied watershed decreased during the simulation period, and no month showed an increase in water yield with a higher temperature.

As might be expected, an increase in precipitation increased water yield, stream flow, and ET. An increase in precipitation will increase runoff thus increasing water yield and stream flow. More available water on the surface and in the rooting zone will increase ET. Higher precipitation amount and intensity did not significantly change the crop growth cycle and irrigation water use, because the majority of rainfall over a year was observed during the dormant season over the San Joaquin Valley. Stream flow rate, indicated by the model prediction at the watershed outlet, was mainly determined by irrigation water use, precipitation, and ET. The study area receives irrigation water from both enclosed rivers and upstream storage outside of the simulation domain. Water diversion from an enclosed river might significantly reduce the stream flow output. For example, 409.8 million m^3 of water from the Merced River was diverted by the Merced Water District during 2004, resulting in an annual average stream flow decrease from 27.4 $m^3 s^{-1}$ at the inlet (USGS gauge #11270900) to only 7.7 $m^3 s^{-1}$ at the subbasin outlet (Luo et al., 2008). Therefore, there was general negative correlation between irrigation water use and stream flow predicted under various scenarios with elevated temperatures (Table 4). For example, predicted irrigation water use in August would decrease by approximately 38.0 mm with temperature increased by 6.4 °C, while approximately a 6.0 $m^3 s^{-1}$ increase of stream flow would be simulated at the same periods.

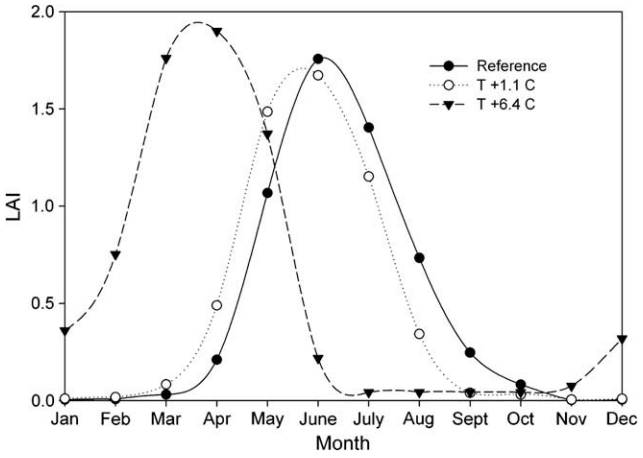

Fig. 7. Change of watershed-wide average leaf area index (LAI) during the simulation period for an increase of 1.1 and 6.4 °C, relative to reference scenario.

Increasing atmospheric CO_2 concentrations had a significant effect on ET, which can be explained by the decrease of stomatal conductance as atmospheric CO_2 increases, resulting in a reduction of plant transpiration. Less crop transpiration decreases irrigation water use. If less water is being used by the crop, farmers will require less irrigation water. This allows for more runoff and therefore a greater water yield and stream flow. Irrigation decreased with an increase in atmospheric CO_2 and temperature. This can be explained by an overall decrease in plant-water stress, leading to less irrigation use. The results indicate that increases in temperature causes an increase in irrigation water use for the winter and spring months and a decrease in irrigation water use for the summer and fall months (Fig. 5). For the increased-CO_2 scenarios with temperature increases, however, the irrigation water use is significantly less ($\alpha = 0.05$). For example, an increase of 6.4 °C with a 330 ppm CO_2 concentration in April causes a 106% increase in irrigation water use. For the same temperature increase with increases in CO_2 by 550 and 970 ppm, the irrigation water use decreases to −0.9% and −30% compared to the reference scenario, respectively. From these results, it could be hypothesized that increased atmospheric CO_2 concentration may potentially have a stronger effect on plant-water needs than an increased temperature. However, further work needs to done on the CO_2-plant growth algorithm in SWAT to solidify these results.

It is important to re-iterate that the overestimation of stomatal conductance in SWAT due to the assumed inverse linear relationship between stomatal conductance and atmospheric CO_2 for all plant species and the lack of LAI increase with increased CO_2 concentration will result in decreased ET rates and subsequent increases in stream flow and water yield. Therefore, one must take caution when interpreting these results, as an ET overestimation will affect the water yield, irrigation water use and stream flow results involving an increased CO_2 concentration. Previous research by Eckhardt and Ulbrich (2003) using the SWAT-G model (discussed in 'The SWAT hydrological model') found that increasing CO_2 in the original SWAT model overestimated the reduction of stomatal conductance, which then overcompensated the actual effect of temperature rise. Their results showed that decreases in groundwater recharge and stream flow changed from 0.3% and 1.5%, respectively, with the original SWAT model to 3% and 4% with the modified SWAT-G. Eckhardt and Ulbrich (2003) is the only work to date that has analyzed this overestimation within SWAT. In this study, the overestimation may also be significant due to the large variation in land cover and therefore the effect of temperature may be dampened.

Because of the broad simplification of the effects of CO_2 on plant growth included, this analysis is still perhaps too uncertain for detailed water management purposes. However, the results provide a bracketed view of how the hydrologic cycle, particularly water yield, ET, irrigation water use and stream flow, might be affected by changes in climate and CO_2 concentration. Additional work needs to be done in SWAT to incorporate varying stomatal conductance and LAI responses in response to increased atmospheric CO_2 concentrations.

These modeled hydrologic changes may have implications on agricultural management and water quality in the San Joaquin watershed. A shift in irrigation timing due to changes in plant growth and a decrease in ET would cause water resource managers to change their water allotment to meet the farmers' needs. Also, if the crop growth cycle is shifted enough, farmers may implement two harvests within the same year, which would have a significant effect on the hydrologic cycle. Increased runoff would allow for more agricultural pollutant transport into an already polluted San Joaquin River and its tributaries. Conversely, runoff with low contaminant concentrations may lead to dilution of pollutants within the San Joaquin River.

Conclusions

This study illustrated changes in water resources related to potential climate change based on the SWAT model simulation in an agriculturally dominated area of the San Joaquin River watershed. The results in this study indicate that the hydrological system in the study area is very sensitive to climatic variations on a monthly and annual basis. Increasing CO_2 concentration to 970 ppm and temperature to 6.4 °C caused watershed-wide average evapotranspiration, averaged over 50 simulated years, to decrease by 37.5%, resulting in increases of water yield by 36.5% and stream flow by 23.5% compared to the present-day climate. Watershed-wide average ET for the 50 simulation years decreased by 37.5% under the A1FI CO_2 scenario, resulting in increases of water yield by 36.5% and stream flow by 23.5%. Increase of precipitation by ±10% and ±20% generally changed water yield and stream flow proportionally, and had negligible effects on predicted ET and irrigation water use.

The results of this study suggested that temperature change has significant effects on all hydrological elements in the San Joaquin River watershed. These effects might be complicated by the agricultural activities and irrigation water diversion in the study area. Generally, elevated temperature shifted the plant growth pattern and re-distributed ET and irrigation water demand over months. Watershed-wide averages of water yield were decreased for all months when temperature was increased alone. However, stream flow rates were significantly increased during summer months due to reduced irrigation water diversion during those months. The quantitative information would allow appropriate decisions on agricultural management and natural resource conservation in this area. This study pointed to the need for a more extensive assessment of potential climate change impacts on the hydrology and agricultural production in agriculturally dominated watersheds.

References

Aber, J.D., Ollinger, S.V., Federer, C.A., Reich, P.B., Goulden, M.L., Kicklighter, D.W., Melillo, J.M., Lathrop Jr., R.G., 1995. Predicting the effects of climate change on water yield and forest production in the northeastern United States. Climate Research 5, 207–222.

Allen, M.R., Ingram, W.J., 2002. Constraints on future changes in climate and the hydrologic cycle. Nature 419 (6903), 224–232.

Arnell, N.W., Liv, C., 2001. Hydrology and water resources. In: McCarthy, J.J., Canziani, O.F., Leary, N.A., Dokken, D.J., White, K.S. (Eds.), Climate Change 2001:

Impacts. Adaptation and Vulnerability. Cambridge University Press, Cambridge, UK, pp. 191–233.
Arnold, J.G., Srinivasan, R., Muttiah, R.S., Williams, J.R., 1998. Large area hydrologic modeling and assessment part I: model development. Journal of the American Water Resources Association 34 (1), 73–89.
Boswell, V.G., 1926. The influence of temperature upon the growth and yield of garden peas. Proceedings of the American Society for Horticultural Science 23, 162–168.
Brekke, L.D., Miller, N.L., Bashford, K.E., Quinn, N.W.T., Dracup, J.A., 2004. Climate change impacts uncertainty for water resources in the San Joaquin River Basin, California. Journal of the American Water Resources Association 40 (1), 149–164.
California Department of Water Resources (DWR), 2007. Land Use Survey Data.
California Environmental Protection Agency (CEPA), 2007. CEPA, Surface Water Database, California Environmental Protection Agency.
California Regional Water Quality Control Board (CRWQCB), 2000. Central Valley Region. Monitoring Data included from the following testing programs: UC Davis Phase II, East San Joaquin Water Quality Coalition, San Joaquin County and Delta Water Quality Coalition, and Westside San Joaquin River Watershed Coalition.
California State Water Resources Control Board, 2002. CWA Section 303(d) List of Water Quality Limited Segments. <http://www.waterboards.ca.gov/tmdl/303d_lists.html> (accessed 8.11.06).
Cayan, D.R., Maurer, E.P., Dettinger, M.D., Tyree, M., Hayhoe, K., 2008. Climate change scenarios for the California region. Climatic Change 87 (Suppl. 1), S21–S42.
Chaplot, V., 2007. Water and soil resources response to rising levels of atmospheric CO_2 concentration and to changes in precipitation and air temperature. Journal of Hydrology 337 (1–2), 159–171.
Chen, 2001. Impacts of Stomatal Resistance on Evapotranspiration and Water Yield in Climate Change Modeling. M.S. Thesis, Washington State University, Pullman, Washington, p. 110.
Crepeau, K.L., Kuivila, K.M., Domagalski, J.L., 1991. River inputs of pesticide to the Sacramento–San Joaquin Delta, CA (Abstract).
Cruise, J.F., Limaye, A.S., Al-Abed, N., 1999. Assessment of impacts of climate change on water quality in the southeastern United States. Journal of the American Water Resources Association 35 (6), 1539–1550.
Dettinger, M.D., Cayan, D.R., Meyer, M.K., Jeton, A.E., 2004. Simulated hydrologic responses to climate variations and change in the Merced, Carson, and American River Basins, Sierra Nevada, California, 1900–2099. Climatic Change 62 (1), 283–317.
Dracup, J.A., Pelmulder, S.D., 1993. Estimation of Monthly Average Streamflow for the Sacramento-San Joaquin River System under Normal, Drought, and Climate Change Conditions. Integrated Modeling of Drought and Global Warming: Impacts on Selected California Resources Report by the National Institute for Global Environmental Change, University of California, Davis, CA, p.112.
Easterling, W.E., Rosenberg, N.J., McKenney, M.S., Allan Jones, C., Dyke, P.T., Williams, J.R., 1992. Preparing the erosion productivity impact calculator (EPIC) model to simulate crop response to climate change and the direct effects of CO_2. Agricultural and Forest Meteorology 59, 17–34.
Eckhardt, K., Ulbrich, U., 2003. Potential impacts of climate change on groundwater recharge and streamflow in a central European low mountain range. Journal of Hydrology 284 (1–4), 244–252.
Field, C.B., Jackson, R.B., Mooney, H.A., 1995. Stomatal responses to increased CO_2: implications from the plant to the global scale. Plant Cell Environment 18, 1214–1225.
Flay, R.B., Narasimhan, T.N., 2000. Application of the soil and water assessment tool (SWAT) and geographic information systems (GIS) to integrated water management of the San Joaquin River Basin, California. Eos, Transactions, AGU 81 (48) (Fall Meet. Suppl., Abstract H21F-06).
Flugel, W., 1995. Delineating hydrologic response units by geographical information-system analyses for regional hydrological modeling using PRMS/MMS in the drainage-basin of the River BROL, Germany. Hydrologic Processes 9, 423–436.
Foe, C., 1990. Detection of pesticides in the San Joaquin watershed during February, 1990. Staff Memorandum, Central Valley Regional Water Quality Control Board, Sacramento, CA.
Foe, C., Connor, V., 1991. San Joaquin Watershed Bioassay Results, 1988–1990. Staff Report. Central Valley Regional Water Quality Control Board, Sacramento, CA.
Foe, C., Sheipline, R., 1993. Pesticide in surface water from applications on orchards and alfalfa during the winter and spring of 1991–1992. Central Valley Regional Water Quality Control Board, Sacramento, CA.
Fontaine, T.A., Klassen, J.F., Hotchkiss, R.H., 2001. Hydrological response to climate change in the Black Hills of South Dakota, USA. Hydrological Sciences 46 (1), 27–40.
Gleick, P.H., 1987. Regional hydrologic consequences of increases in atmospheric CO_2 and other trace gases. Climatic Change 10 (2), 137–160.
Hanratty, M.P., Stefan, H.G., 1998. Simulating climate change effects in a Minnesota agricultural watershed. Journal of Environmental Quality 27 (6), 1524–1532.
Hay, L.E., Wilby, R.L., Leavesley, G.H., 2000. A comparison of delta change and downscaled GCM scenarios for three mountainous basins in the United States. Journal of the American Water Resources Association 36 (2), 387–397.
Hendry, G.R., Lewin, K.F., Nagy, K.F., 1993. Free air carbon dioxide enrichment: development, progress, results. Vegatatio 104/105, 17–31.
IPCC, 2001. Climate Change. The Physical Science Basis. Cambridge, UK: Cambridge University Press. 996 p.
IPCC, 2001. Special Report on Emission Scenarios. Cambridge University Press, 612 p.
IPCC, 2007. Climate Change 2007: The Physical Science Basis. Contribution of Working Group I to the Fourth Assessment Report of the Intergovernmental Panel on Climate Change. Cambridge University Press, Cambridge, United Kingdom and New York, NY, USA.
Kalnay, E., Cai, M., 2003. Impact of urbanization and land-use change on climate. Nature 423, 528–531.
Kamga, F.M., 2001. Impact of greenhouse gas induced climate change on the runoff of the Upper Benue River (Cameroon). Journal of Hydrology 252, 145–156.
Knisel, W.G., 1980. CREAMS: a field scale model for chemicals, runoff, and erosion from agricultural management systems. USDA Technical Bulletin, 643.
Knowles, N., Cayan, D., 2002. Potential effects of global warming on the Sacramento/San Joaquin watershed and the San Francisco estuary. Geophysical Research Letters 19 (18), 1891.
Kratzer, C.R., 1999. Transport of Diazinon in the San Joaquin River Basin, California. Journal of the American Water Resources Association 35 (2), 379–395.
Labat, D., Godderis, Y., Probst, J.L., Guyot, J.L., 2004. Evidence for global runoff increase related to climate warming. Advances in Water Resources 27 (6), 631–642.
LaDochy, S., Medina, R., Patzert, W., 2007. Recent California climate variability: spatial and temporal patterns in temperature trends. Climate Research 33, 159–169.
Leavesley, 1983. Precipitation-Runoff Modeling System: User's Manual. US Geological Survey, Denver, CO, USA.
Legesse, D., Vallet-Coulomb, C., Gasse, F., 2003. Hydrological response of a catchment to climate and land use changes in Tropical Africa: case study South Central Ethiopia. Journal of Hydrology 275 (1–2), 67–85.
Lettenmaier, D., Gan, T., 1990. Hydrologic sensitivities of the Sacramento-San Joaquin River basin, California, to global warming. Water Resources Research 26, 69–86.
Lettenmaier, D.P., Wood, A.W., Palmer, R.N., Wood, E.F., Stakhiv, E.Z., 1999. Water resources implications of global warming: a US regional perspective. Climatic Change 43 (3), 537–579.
Luedeling, E., Zhang, M., Luedeling, V., Girvetz, E.H., in press. Sensitivity of winter chill models for fruit and nut trees to climatic changes expected in California's Central Valley. Agriculture, Ecosystems and Environment, doi:10.1016/j.agee.2009.04.016.
Luo, Y., Zhang, X., Liu, X., Ficklin, D., Zhang, M., 2008. Dynamic modeling of organophosphate pesticide load in surface water in the northern San Joaquin Valley watershed of California. Environmental Pollution 156, 1171–1181.
Magoon, C.A., Culpepper, C.W., 1932. Response of sweet corn to varying temperatures from time of planting to canning maturity. USDA Technical Bulletin, 312.
Maurer, E., Duffy, P.B., 2005. Uncertainty in projections of streamflow changes due to climate change in California. Geophysical Research Letters, 32.
Maurer, E., 2007. Uncertainty in hydrologic impacts of climate change in the Sierra Nevada, California, under two emissions scenarios. Climatic Change 82 (3), 309–325.
Medlyn, B.E., Barton, C.V.M., Broadmeadow, M.S.J., Ceulemans, R., De Angelis, P., Forstreuter, M., Freeman, M., Jackson, S.B., Kellomaki, S., Laitat, E., Rey, A., Roberntz, P., Sigurdsson, B.D., Strassemeyer, J., Wang, K., Curtis, P.S., Jarvis, P.G., 2001. Stomatal conductance of forest species after long-term exposure to elevated CO_2 concentrations: a synthesis. New Phytologist 149, 247–264.
Miller, N.L., Kim, J., Hartman, R.K., Farrara, J., 1999. Downscaled climate and streamflow study of the Southwest United States. Journal of the American Water Resources Association 35 (6), 1525–1537.
Miller, N.L., Kim, J., 2000. Climate change sensitivity analysis for two California watersheds: addendum to the downscaled climate and streamflow study of the Southwest United States. Journal of the American Water Resources Association 36 (3), 657–661.
Morison, J.I.L., Gifford, R.M., 1983. Stomatal sensitivity to carbon dioxide and humidity. Plant Physiology 71, 789–796.
Morison, J.I.L., 1987. Intercellular CO_2 Concentration and Stomatal Response to CO_2. Stomatal Function. Stanford University Press, Stanford CA. 229–251.
Nash, J.E., Sutcliffe, J.V., 1976. River flow forecasting through conceptual models: part I. A discussion of principles. Journal of Hydrology 10 (1976), 282–290.
Nash, L.L., Gleick, P.H., 1991. Sensitivity of streamflow in the Colorado Basin to climatic changes. Journal of Hydrology 125 (3–4), 221–241.
Nash, L.L., Gleick, P.H., 1993. Colorado River Basin and Climatic Change. The sensitivity of streamflow and Water Supply to Variations in Temperature and Precipitation. Pacific Institute for Studies in Development, Environment and Security, Oakland, CA. PB-94-128527/XAB.
National Oceanic and Atmospheric Administration (NOAA). National Climatic Data Center (accessed 15.05.08).
Nietsch, S.L., Arnold, J.G., Kiniry, J.R., Williams, J.R., King, K.W., 2005. Soil and Water Assessment Tool Theoretical Documentation. Version 2005. College Station, TX: Texas Water Resource Institute.
Pritchard, S.G., Rogers, H.H., Prior, S.A., Peterson, C.M., 1999. Elevated CO_2 and plant structure: a review. Global Change Biology 5, 807–837.
Racsko, P., Szeidl, L., Semenov, M., 1991. A serial approach to local stochastic weather models. Ecological Modelling 57 (1–2), 27–41.
Rind, D., Goldberg, R., Hansen, J., Rosenzweig, C., Ruedy, R., 1990. Potential evapotranspiration and the likelihood of future drought. Journal of Geophysical Research 95 (D7), 9983–10004.

Rosenberg, N.J., Epstein, D.J., Wang, D., Vail, L., Srinivasan, R., Arnold, J.G., 1999. Possible impacts of global warming on the hydrology of the Ogallala aquifer region. Climatic Change 42 (4), 677–692.

Saxe, H., Ellsworth, D.S., Heath, J., 1998. Trees and forest functioning in an enriched CO_2 atmosphere. New Phytologist 139, 395–436.

Schaake, J.C., 1990. Water resources. In: Waggoner, P.E. (Ed.), Water Resources. John Wiley, New York, pp. 177–206 (Chapter 8).

Schuol, J., Abbaspour, K.C., Srinivasan, R., Yang, H., 2008. Estimation of freshwater availability in the West African sub-continent using the SWAT hydrologic model. Journal of Hydrology 352 (1–2), 30–49.

Semenov, M.A., Barrow, E.M., 1997. Use of a stochastic weather generator in the development of climate change scenarios. Climatic Change 35 (4), 397–414.

Semenov, M.A., Brooks, R.J., Barrow, E.M., Richardson, C.W., 1998. Comparison of WGEN and LARS-WG stochastic weather generators for diverse climates. Climate Research 10, 95–107.

Sharpley, A.N, Williams, J.R., 1990. Erosion/Productivity Impact Calculator, 1. Model Documentation. USDA–ARS Technical Bulletin 1768.

Soil Conservation Service, 1984. SCS National Engineering Handbook. US Department of Agriculture, Washington, DC.

Srinivasan, R., Ramanarayanan, T.S., Arnold, J.G., Bednarz, S.T., 1998. Large area hydrologic modeling and assessment part II: model application. Journal of the American Water Resources Association 34 (1), 91–101.

Stonefelt, M.D., Fontaine, T.A., Hotchkiss, R.H., 2000. Impacts of climate change on water yield in the upper Wind River Basin. Journal of the American Water Resources Association 36 (2), 321–336.

Tyree, M.T., Alexander, J.D., 1993. Plant water relations and the effects of elevated CO_2: a review and suggestions for future research. Plant Ecology 104–105 (1), 47–62.

USBR (US Bureau of Reclamation), 1991. Evaluation of Central Valley Project Water Supply and Delivery Systems. Technical Report by the USBR Mid-Pacific Regional Office, Sacramento, CA.

USDA, 2007. Soil Survey Geographic (SSURGO) Database, United States Department of Agriculture.

USEPA (US Environmental Protection Agency), 1997. Climate Change and California. Report No. 230-F-97-008e, USEPA Office of Policy, Planning, and Evaluation, Washington, DC.

USEPA, 2002. Guidance for Selecting Input Parameters in Modeling the Environmental Fate and Transport of Pesticides, Version II. Office of Pesticide Programs, US Environmental Protection Agency.

USEPA, 2004. Pesticide Root Zone Model (PRZM) Field and Orchard Crop Scenarios: Guidance for Selecting Field Crop and Orchard Scenario Input Parameters. Office of Pesticide Programs, US Environmental Protection Agency.

USEPA, 2007. Data for the Better Assessment Science Integrating Point and Nonpoint Sources (BASINS) Model, United States Environmental Protection Agency.

USEPA, 2008. Impaired and Threatened Water Lists. <http://www.epa.gov/region09/water/tmdl/303d.html> (accessed 11.10.08).

USGS, 2007. National Water Information System: Web Interface, United States Geographical Survey.

VanRheenen, N.T., Wood, A.W., Palmer, R.N., Lettenmaier, D.P., 2004. Potential implications of PCM climate change scenarios for Sacramento-San Joaquin River Basin hydrology and water resources. Climatic Change 62 (1), 257–281.

Wand, S.J.E., Midgley, G.F., Jones, M.H., Curtis, P.S., 1999. Responses of wild C4 and C3 grass (Poaceae) species to elevated atmospheric CO_2 concentrations: a meta-analytic test of current theories and perceptions. Global Change Biology 5, 723–741.

Wilby, R., Dettinger, M., 2003. Streamflow changes in the Sierra Nevada, California, simulated using a statistically downscaled general circulation model scenario of climate change. Linking Climate Change to Land Surface Change, 99–121.

Wolock, D.M., McCabe, G.J., 1999. Estimates of runoff using water-balance and atmospheric general circulation models. Journal of the American Water Resources Association 35 (6), 1341–1350.

Wullschleger, S.D., Gunderson, C.A., Hanson, P.J., Wilson, K.B., Norby, R.J., 2002. Sensitivity of stomatal and canopy conductance to elevated CO_2 concentration-interacting variables and perspectives of scale. New Phytologist 153, 319–331.

Yates, D.N., 1996. WatBal: an integrated water balance model for climate impact assessment of river basin runoff. International Journal of Water Resources Development 2, 121–139.

Zhu, T., Jenkins, M.W., Lund, J.R., 2005. Estimated impacts of climate warming on California water availability under twelve future climate scenarios. Journal of the American Water Resources Association 41 (5), 1027–1038.